International Journal of Heat and Mass Transfer 82 (2015) 309–315

Contents lists available at ScienceDirect

International Journal of Heat and Mass Transfer

journal homepage: www.elsevier.com/locate/ijhmt

Effects of Soret diffusion on spherical flame initiation and propagation

Wang Han [a], Zheng Chen [a,b,*]

[a] SKLTCS, Department of Mechanics and Engineering Science, College of Engineering, Peking University, Beijing 100871, China
[b] Department of Aeronautics and Astronautics, College of Engineering, Peking University, Beijing 100871, China

ARTICLE INFO

Article history:
Received 17 August 2014
Received in revised form 12 November 2014
Accepted 18 November 2014

Keywords:
Soret diffusion
Spherical flame propagation
Markstein length
Ignition

ABSTRACT

Dynamics of spherical flame initiation and propagation with Soret diffusion are investigated using large-activation-energy asymptotic analysis. Under the assumptions of constant density and quasi-steady flame propagation, a general correlation between the flame propagating speed and flame radius considering Soret diffusion and external energy deposition is derived. Emphasis is placed on assessing the effects of Soret diffusion on spherical flame propagation speed, Markstein length, and critical ignition condition. The stretched flame speed is found to be increased and reduced by the Soret diffusion of light and heavy fuels, respectively. For both light and heavy fuels, the absolute value of Markstein length increases after including Soret diffusion, indicating that premixed flames become more sensitive to stretch rate with Soret diffusion. It is found that the Markstein length can be characterized by an effective Lewis number which includes the effects of Soret diffusion. Moreover, Soret diffusion is shown to affect the ignition process since the spherical flame kernel is highly stretched. For large hydrocarbon fuels with high Lewis numbers, the minimum ignition power becomes much larger after considering Soret diffusion.

1. Introduction

The successful ignition of a static pre-mixture is determined by the evolution of the ignition kernel. The ignition kernel is highly curved and stretched. Its propagation is controlled by the stretch effects coupling with the preferential diffusion between heat and mass (i.e. the Lewis number effect) [1,2]. Therefore, critical ignition condition strongly depends on the Lewis number of the deficient reactant [3–9]. Specifically, due to the high positive stretch rate of the ignition kernel, the minimum ignition energy and critical ignition radius increase significantly with the Lewis number [6–9].

In most of previous studies on ignition and spherical flame propagation, the mass transport was represented by Fickian diffusion (mass diffusion due to concentration gradient) while little attention was paid to Soret diffusion (mass diffusion due to temperature gradient). In the presence of very light or heavy species and steep temperature gradient, Soret diffusion, which drives light (heavy) species toward (away from) the hot zone, is also important for the mass transport [10]. In a spark ignition process, the temperature inside the ignition kernel after spark discharge is very high and thus there exists large temperature gradient. It is therefore expected that ignition and flame kernel propagation are influenced by the Soret diffusion.

In the literature, Soret diffusion in combustion has been mainly studied through numerical simulation. For examples, the Soret diffusion of heavy species such as particle and soot was investigated by Rosner and coworkers [11,12]; the influence of Soret diffusion on flame extinction was analyzed by Ern and Giovangigli [13,14] and Law and coworkers [15,16]; the Soret diffusion effects on laminar flame speed were assessed by Bongers and de Goey [17] and Yang et al. [18]. The readers are referred to Refs. [18,19] for a summary of previous studies on this subject. Recently, Liang et al. [20,21] have examined the Soret diffusion effects on the ignition and propagation of H_2/CO/air flames through numerical simulation with detailed chemistry and transport. It was found that the minimum ignition energy and stretched flame speed are greatly affected by the Soret diffusion [20,21].

The numerical studies [11–21] mentioned above indicated discernable effects of Soret diffusion in combustion with species that are very light or very heavy. Unfortunately, numerical simulation is usually constrained to specific fuel and hence the conclusion is lack of generality. Unlike simulation, theoretical analysis is helpful for general understanding of the physical insight into the problem. However, there are only a few theoretical studies on Soret effects in the literature. Garcia-Ybarra et al. [22,23] studied the Soret diffusion effects on thermo-diffusive stability limits and Markstein lengths of premixed flames. Arias-Zugasti and Rosner [24] assessed

---

* Corresponding author at: SKLTCS, Department of Mechanics and Engineering Science, College of Engineering, Peking University, Beijing 100871, China. Tel.: +86 10 62766232.

E-mail address: cz@pku.edu.cn (Z. Chen).

http://dx.doi.org/10.1016/j.ijheatmasstransfer.2014.11.062
0017-9310/

the influence of Soret diffusion on counterflow diffusion flames. Fong et al. [25] examined the Soret diffusion effects on laminar diffusion flame in high density fluids. In these studies [22–25], only the planar flame was analyzed. However, in the literature there is no theoretical analysis on premixed spherical flame kernel development.

Therefore, the objectives of this study are to provide a theoretical description of premixed spherical flames with Soret diffusion and to assess the effects of Soret diffusion on spherical flame initiation and propagation. In the following, we shall first introduce the theoretical model and derive a correlation describing the spherical flame initiation and propagation with Soret diffusion based on the quasi-steady and large-activation-energy assumptions (the chemical source term is not solved, but is approximated by the corresponding jump conditions across the flame). Then, based on this correlation, we shall examine the effects of Soret diffusion on stretched flame speed, Markstein length, and critical ignition condition.

2. Theoretical analysis

2.1. Mathematical model

Similar to our previous study [6], one-dimensional, adiabatic spherical flame initiation and propagation are considered in the theoretical analysis. Due to its simple geometry and well defined stretch rate, the spherical propagating flame is generally employed to measure the laminar flame speed [26–35], especially at high pressures [36–39]. As shown in Fig. 1, a self-sustained outwardly propagating spherical flame can be established through successful ignition at the center of a quiescent homogeneous combustible mixture. The flame structure consists of a burned gas zone, a thin reaction zone (which is considered as a flame sheet at large-activation energy), and an unburned zone.

One-step, first-order, global reaction model is employed. Therefore, the coupling between Soret diffusion flux and elementary reaction rates [20] is not included in the present model and we focus on the transport effects. The mixture is assumed to be deficient in fuel and thus only fuel concentration needs to be considered. For the sake of simplicity, we employ the diffusive-thermal model [1,40], according to which the density is constant and the flow is static without convection. In a one-dimensional spherical coordinate, the governing equations for temperature $\tilde{T}$ and fuel mass fraction $\tilde{Y}$ are

$$\tilde{\rho}\tilde{C}_P\frac{\partial\tilde{T}}{\partial\tilde{t}}=\frac{1}{\tilde{r}^2}\frac{\partial}{\partial\tilde{r}}\left(\tilde{r}^2\tilde{\lambda}\frac{\partial\tilde{T}}{\partial\tilde{r}}\right)+\tilde{q}\tilde{\omega} \tag{1}$$

$$\tilde{\rho}\frac{\partial\tilde{Y}}{\partial\tilde{t}}=-\frac{1}{\tilde{r}^2}\frac{\partial}{\partial\tilde{r}}(\tilde{r}^2\tilde{j}_Y)-\tilde{\omega} \tag{2}$$

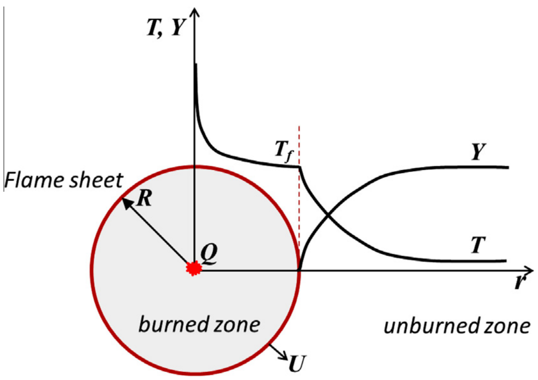

Fig. 1. Schematization of the spherical flame structure.

with

$$\tilde{\omega}=\tilde{\rho}\tilde{A}\tilde{Y}\exp\left(-\frac{\tilde{E}}{\tilde{R}^0\tilde{T}}\right) \tag{3}$$

where $\tilde{t}$ and $\tilde{r}$ are temporal and spatial coordinate, respectively. The density $\tilde{\rho}$, heat capacity $\tilde{C}_P$, and heat conductivity $\tilde{\lambda}$ of the mixture are all assumed to be constant in the diffusive-thermal model. The parameter, $\tilde{q}$, denotes the reaction heat-release per unit mass of fuel. $\tilde{A}$ is the pre-factor of Arrhenius law, $\tilde{E}$ the activation energy, and $\tilde{R}^0$ the universal gas constant.

The mixture-averaged diffusion model [10,17,25] is employed and the diffusive mass flux in Eq. (2) is

$$\tilde{j}_Y=-\tilde{\rho}\tilde{D}\left(\frac{\partial\tilde{Y}}{\partial\tilde{r}}+\alpha\tilde{Y}\frac{\partial\tilde{T}}{\tilde{T}\partial\tilde{r}}\right) \tag{4}$$

in which the first term on the right hand side represents Fickian diffusion while the second term corresponds to Soret diffusion. $\tilde{D}$ denotes the molecular diffusivity of fuel and α is the Soret coefficient which is negative for light species (hydrogen) and positive for heavy fuels (e.g. *n*-heptane, *n*-decane) [17,25].

Similar to our previous study [6], a constant energy flux, $\tilde{Q}$, is locally deposited at the center to initialize the ignition kernel.

$$-\left(4\pi\tilde{r}^2\tilde{\lambda}\frac{\partial\tilde{T}}{\partial\tilde{r}}\right)_{\tilde{r}\to 0}=\tilde{Q} \tag{5}$$

This is a limitation of theoretical analysis since in practice the ignition energy deposition should be resolved in time and space. The employment of such a steady-state energy deposition is for the purpose to obtain analytical solution [6]. Nevertheless, as demonstrated by numerical simulation [6], this simplification does not prevent the model from predicting qualitatively correct results.

We introduce the following non-dimensional variables

$$t=\frac{\tilde{t}}{\tilde{\delta}_f^0/\tilde{S}_u^0},\quad r=\frac{\tilde{r}}{\tilde{\delta}_f^0},\quad u=\frac{\tilde{u}}{\tilde{S}_u^0},\quad T=\frac{\tilde{T}-\tilde{T}_u}{\tilde{T}_{ad}-\tilde{T}_u},\quad Y=\frac{\tilde{Y}}{\tilde{Y}_u} \tag{6}$$

where $\tilde{T}_u$ and $\tilde{Y}_u$ denote the temperature and fuel mass fraction in the fresh mixture. The characteristic speed $\tilde{S}_u^0$, characteristic length $\tilde{\delta}_f^0=\tilde{\lambda}/(\tilde{\rho}\tilde{C}_P\tilde{S}_u^0)$, and characteristic temperature $\tilde{T}_{ad}=\tilde{T}_u+\tilde{Y}_u\tilde{q}/\tilde{C}_P$ are, respectively, the laminar flame speed, flame thickness, and flame temperature of an adiabatic planar flame. We study spherical flame initiation and propagation in the coordinate attached to the moving flame front, $R=R(t)$. In this coordinate, $\xi=r-R(t)$, the flame can be considered as in a quasi-steady state (the validation of this quasi-steady assumption has been demonstrated by transient numerical simulation [6,8,9]) and thereby the non-dimensional governing equations become

$$-U\frac{dT}{d\xi}=\frac{1}{(\xi+R)^2}\frac{d}{d\xi}\left[(\xi+R)^2\frac{dT}{d\xi}\right]+\omega \tag{7}$$

$$-U\frac{dY}{d\xi}=\frac{Le^{-1}}{(\xi+R)^2}\frac{d}{d\xi}\left[(\xi+R)^2\left(\frac{dY}{d\xi}+\frac{\alpha Y}{\gamma+T}\cdot\frac{dT}{d\xi}\right)\right]-\omega \tag{8}$$

with

$$\omega=\frac{1}{2Le}\cdot Y\cdot Z^2\cdot\exp\left[\frac{Z(T-1)}{\sigma+(1-\sigma)T}\right] \tag{9}$$

where U is the non-dimensional flame propagation speed, $U=dR(t)/dt$, Le the Lewis numbers, $Le=\tilde{\lambda}/(\tilde{\rho}\tilde{C}_P\tilde{D})$, γ the temperature ratio, $\gamma=\tilde{T}_u/(\tilde{T}_{ad}-\tilde{T}_u)$. Z is the Zel'dovich number, $Z=\tilde{E}(1-\sigma)/\tilde{R}^0\tilde{T}_{ad}$ and σ the thermal expansion ratio, $\sigma=\tilde{T}_u/\tilde{T}_{ad}$.

The boundary conditions for temperature and fuel mass fraction are

$$\xi = -R, \quad (\xi + R)^2 \frac{dT}{d\xi} = -Q, \quad \frac{dY}{d\xi} = 0 \tag{10}$$

$$\xi \to \infty, \quad T = 0, \quad Y = 1 \tag{11}$$

where Q is the normalized ignition power given by

$$Q = \frac{\widetilde{Q}}{4\pi \tilde{\lambda} \tilde{\delta}_f^0 (\widetilde{T}_{ad} - \widetilde{T}_u)} \tag{12}$$

2.2. Analytical solution

In the limit of large activation energy, chemical reaction occurs only within a very thin zone of high temperature and at the flame sheet (i.e., $\xi = 0$) the jump relations for the non-dimensional temperature and mass fraction are given by [40–43]

$$Y|_{\xi=0^+} = Y|_{\xi=0^-} = 0, \quad T|_{\xi=0^+} = T|_{\xi=0^-} = T_f \tag{13}$$

$$\begin{aligned} \left.\frac{dT}{d\xi}\right|_{\xi=0^-} - \left.\frac{dT}{d\xi}\right|_{\xi=0^+} &= \frac{1}{Le}\left(\left.\frac{dY}{d\xi}\right|_{\xi=0^+} - \left.\frac{dY}{d\xi}\right|_{\xi=0^-} \right) \\ &= [\sigma + (1-\sigma)T_f]^2 \exp\left[\frac{Z}{2} \frac{T_f - 1}{\sigma + (1-\sigma)T_f} \right] \end{aligned} \tag{14}$$

With these jump conditions, Eqs. (7) and (8) together with conditions given by Eqs. (10) and (11) can be solved analytically in the unburned ($\xi \geqslant 0$) and burned ($-R \leqslant \xi \leqslant 0$) zones. The analytical solution to the temperature distribution is

$$T(\xi) = \begin{cases} T_f + Q \cdot e^{-UR} \int_\xi^0 (\tau + R)^{-2} e^{-U\tau} d\tau & \text{for} \quad -R \leqslant \xi \leqslant 0 \\ T_f I(\xi, U)/I(0, U) & \text{for} \quad \xi \geqslant 0 \end{cases} \tag{15}$$

where $I(x, \kappa) = \int_x^\infty (\kappa + R)^{-2} \exp(-\kappa\tau) d\tau$ and T_f is the flame temperature to be determined later. According to Eq. (15), the temperature gradient at the flame sheet on the side of the burned gas can be obtained as follows

$$\left.\frac{dT}{d\xi}\right|_{0^-} = -R^{-2} \cdot e^{-UR} \cdot Q \tag{16}$$

which implies that the effect of the ignition power decays exponentially with the flame radius.

For the fuel-lean case, the fuel mass fraction in the burned gas zone ($-R \leqslant \xi \leqslant 0$) is zero and that in the unburned gas zone ($\xi \geqslant 0$) is obtained by solving Eq. (8), which is written in the following form

$$\frac{d^2Y}{d\xi^2} + \left(LeU + \frac{2}{\xi + R} \right) \frac{dY}{d\xi} + \alpha \left[\frac{d(Yf)}{d\xi} + \frac{2}{\xi + R} Yf \right] = 0 \tag{17}$$

In the above equation, f represents the "driving force" of Soret diffusion [15,18]

$$f = \frac{1}{\gamma + T} \cdot \frac{dT}{d\xi} = \frac{-T_f(\xi + R)^{-2} e^{-U\xi}}{\gamma I(0, U) + T_f I(\xi, U)} \quad \text{with} \quad \gamma = \sigma/(1 - \sigma) \tag{18}$$

which can be evaluated using the temperature distribution in the unburned zone ($\xi \geqslant 0$) given by Eq. (15). It is noted that we always have $f < 0$ since the temperature gradient in unburned gas is negative.

Soret diffusion is usually one-order smaller than Fickian diffusion, indicating that the Soret coefficient is much less than unity (i.e. $|\alpha| \ll 1$). Therefore, Eq. (17) can be solved in an asymptotic manner. By neglecting the second and higher order terms of $O(\alpha^2)$, we obtain the following asymptotic expression for fuel mass fraction in the unburned zone

$$Y = Y_0 + \alpha Y_1 + O(\alpha^2) \text{ for } \xi \geqslant 0 \tag{19}$$

where

$$Y_0(\xi) = 1 - I(\xi, ULe)/I(0, ULe) \tag{20}$$

$$Y_1(\xi) = -\frac{I(\xi, ULe)}{I(0, ULe)} \cdot \int_0^\infty \frac{F(\tau) \cdot Y_0(\tau)}{dY_0(\tau)/d\tau} d\tau + \int_\xi^\infty \frac{F(\tau)[Y_0(\tau) - Y_0(\xi)]}{dY_0(\tau)/d\tau} d\tau \tag{21}$$

with $F(\xi) = -\frac{d(Y_0 f)}{d\xi} - \frac{2Y_0 f}{\xi + R}$.

Substituting Eqs. (15), (19)–(21) into the jump relations in Eq. (14), we obtain the following algebraic system of equations for flame propagation speed U, flame radius R, and flame temperature T_f

$$\begin{cases} T_f \frac{R^{-2} e^{-UR}}{\int_R^\infty \tau^{-2} e^{-U\tau} d\tau} - QR^{-2} e^{-UR} = \frac{1}{Le} \frac{R^{-2} e^{-ULeR}}{\int_R^\infty \tau^{-2} e^{-ULe\tau} d\tau} \left[1 + \alpha \int_0^\infty G(\tau) d\tau \right] \\ T_f \frac{R^{-2} e^{-UR}}{\int_R^\infty \tau^{-2} e^{-U\tau} d\tau} - QR^{-2} e^{-UR} = [\sigma + (1-\sigma)T_f]^2 \exp\left[\frac{Z}{2} \cdot \frac{T_f - 1}{\sigma + (1-\sigma)T_f} \right] \end{cases} \tag{22}$$

in which

$$\begin{aligned} G(x) = T_f \frac{I(x, ULe)}{I(0, ULe)} \times \Bigg\{ & \frac{Ue^{ULex - Ux}[I(0, ULe) - I(x, ULe)] - x^{-2} e^{-U(x+R)}}{\gamma I(0, U) + T_f I(x, U)} \\ & - \frac{T_f x^{-2} e^{ULex - 2Ux + UR}[I(0, ULe) - I(x, ULe)]}{[\gamma I(0, U) + T_f I(x, U)]^2} \Bigg\} \end{aligned}$$

In the limit of $R \to \infty$ (i.e. a planar flame), Eq. (22) reduces to $U = T_f = 1$, indicating that the Soret diffusion does not affect the laminar flame speed and flame temperature of an adiabatic planar flame. This is due to the facts that enthalpy conservation is always maintained in the unstretched planar flame whenever the Soret diffusion is included or not, and that the one-step global reaction model is considered which excluding the coupling between Soret diffusion flux and elementary reaction rates [20].

When the Soret diffusion and ignition power are neglected (i.e. $\alpha = 0$, $Q = 0$), Eq. (22) reduces to

$$\begin{aligned} T_f \frac{R^{-2} e^{-UR}}{\int_R^\infty \tau^{-2} e^{-U\tau} d\tau} &= \frac{1}{Le} \frac{R^{-2} e^{-ULeR}}{\int_R^\infty \tau^{-2} e^{-ULe\tau} d\tau} \\ &= [\sigma + (1-\sigma)T_f]^2 \exp\left[\frac{Z}{2} \cdot \frac{T_f - 1}{\sigma + (1-\sigma)T_f} \right] \end{aligned} \tag{23}$$

which is the same as the previous results on spherical flame propagation [41]. Therefore, the present analysis is consistent with results in previous studies in the limit of $\alpha = 0$.

By numerically solving Eq. (22) using Newton's iterative method, we can get the flame propagation speed, U, as a function of R, α, Q, and Le. Therefore, with the help of Eq. (22), the effects of Soret diffusion on spherical flame ignition and propagation can be assessed at different values of Soret coefficient α, ignition power Q, and Lewis number Le.

3. Results and discussion

This study is focused on assessing the Soret diffusion effects on spherical flame initiation and propagation. In the following, the results on stretched flame speed, Markstein length, and minimum ignition power at different values of Soret diffusion coefficients and Lewis numbers are presented. The Zeldovich number, $Z = 10$, and thermal expansion ratio, $\sigma = 0.15$ and $\gamma = \sigma/(1 - \sigma) = 0.1765$, are fixed. We consider two Lewis numbers, $Le = 0.5$ and $Le = 2.0$, which represent light and heavy fuels, respectively. Since the Soret diffusion coefficient, α, is negative/positive for light/heavy species, we choose $\alpha = -0.1$ for $Le = 0.5$ and $\alpha = +0.1$ for $Le = 2.0$. The approximate value of Soret diffusion coefficient is $\alpha = -0.29$ for hydrogen molecule at high temperature [19,44] and its absolute value decreases for hydrogen in the low-temperature preheat zone. As mentioned before, the Soret diffusion coefficient is assumed to be a constant which is a limitation of the present analysis. It is noted that the value of $\alpha = -0.1$ or $\alpha = +0.1$ is somewhat arbitrarily chosen. Nevertheless, the same conclusion can be drawn when other values of α are used since the theory works for all different values of α.

3.1. Influence of Soret diffusion on spherical flame propagation

The spherical flame kernel generated by energy deposition is highly stretched; and its propagation speed depends strongly on the Markstein length which characterizes the variation in local flame speed due to the influence of external stretching [6,8,9]. Therefore, understanding the stretched flame propagation speed and Markstein length is helpful for examining the critical ignition condition. Here we first consider the freely propagating spherical flame without ignition energy deposition at the center (i.e. $Q = 0$).

Figure 2 shows the flame propagation speed, U, and flame temperature, T_f, as a function of flame radius, R, for light and heavy fuels. It is seen that for light fuels (i.e., $Le = 0.5$), the presence of Soret diffusion (i.e., the Soret diffusion coefficient changes from $\alpha = 0$ to $\alpha = -0.1$) increases the flame propagation speed and temperature. This is due to the fact that Soret diffusion drives light fuels to diffuse into the reaction zone with high temperature and hence increases the local equivalence ratio, which makes the flame become stronger. For heavy fuels (i.e. $Le = 2.0$), the opposite situation arises and the values of U and T_f are decreased after considering Soret diffusion (α changes from $\alpha = 0$ to $\alpha = +0.1$). Moreover, the results in Fig. 2 indicate that the smaller the flame radius, the larger the influence of Soret diffusion. Therefore, it is expected that Soret diffusion can significantly affect the spherical flame initiation corresponding to relatively small radius.

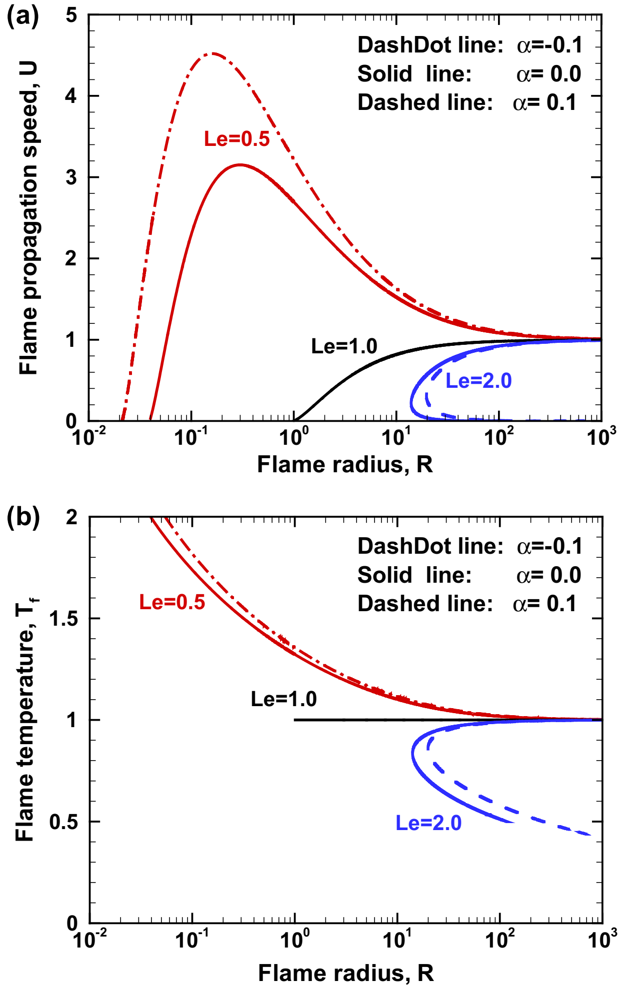

Fig. 2. Change of the (a) flame propagation speed and (b) flame temperature with flame radius.

Figure 3 shows change of the flame propagation speed with flame stretch rate (which is $K = 2U/R$ for outwardly propagating spherical flame). The U–K curves are shown to be strongly affected by Soret diffusion coefficient as well as Lewis number. This is caused by the coupling between the positive stretch rate and preferential diffusion between heat and mass [2]. Moreover, Fig. 3 indicates that U changes linearly with K at small stretch rate. Therefore, the unstretched flame speed, U^0, and Markstein length, L, can be obtained according to the linear relationship of $U = U^0 - L \cdot K$.

As mentioned, the unstretched flame speed, U^0, is not affected by Soret diffusion. However, the Markstein length, L, depends on whether Soret diffusion is included or not. Figure 4 shows that the normalized Markstein length, $L(\alpha)/L(\alpha = 0)$, as a function of Soret diffusion coefficient, α, for $Le = 0.5$ and 2.0. It is observed that the normalized Markstein length increases linearly with the absolute value of Soret diffusion coefficient. This implies that for both light and heavy fuels, the stretched flame speed becomes more sensitive to stretch rate after including Soret diffusion. Furthermore, it is observed that the influence of Soret diffusion on Markstein length of light fuel with $Le = 0.5$ is much stronger that on Markstein length of heavy fuel with $Le = 2.0$. This is due to the fact that the higher flame temperature (see Fig. 2b) and temperature gradient at smaller Lewis number induces stronger Soret diffusion according to Eq. (18).

Since Markstein length is determined at small stretch rate which corresponds to large flame radius (i.e. $R \gg 1$), we consider the spherical flame propagation with large radius, which can be analyzed under the quasi-planar flame assumption ($R \gg 1$) [45]. In the limit of $R \gg 1$, Eq. (22) reduces to

$$\begin{aligned} T_f\left(U + \frac{2}{R}\right) &= U + \frac{2}{LeR}\left(1 + \alpha\int_0^{\infty} H(\tau)d\tau\right) \\ &= [\sigma + (1-\sigma)T_f]^2 \exp\left[\frac{Z}{2}\frac{T_f - 1}{\sigma + (1-\sigma)T_f}\right] \end{aligned} \tag{24}$$

where $H(x) = -T_f(U + 2/R)\{1 - \exp[-(LeU + 2/R)x]\}/\{\gamma\exp[-(U + 2/R)x] + T_f\}$.

Using Taylor expansion for Eq. (24) at $K \ll 1$ (or $R \gg 1$), we obtain the following expression for the Markstein length:

$$L = 1 - \left(\frac{Z}{2} - 2\sigma + 1\right)\left(\frac{1}{Le'} - 1\right) \tag{25}$$

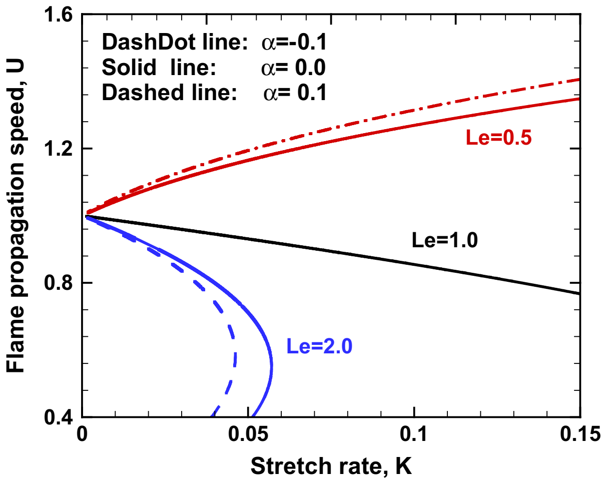

Fig. 3. Change of the flame propagation speed with stretch rate.

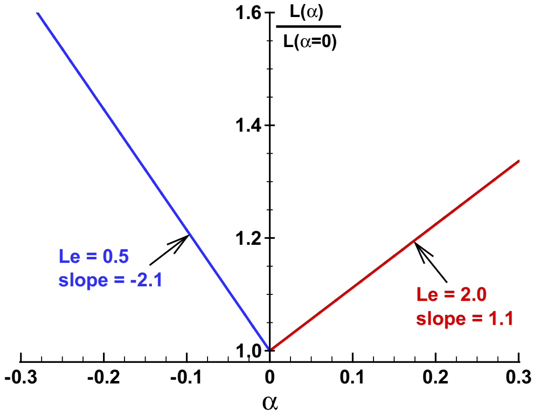

Fig. 4. The normalized Markstein length as a function of Soret diffusion coefficient. $L(\alpha = 0) = -4.7$ for $Le = 0.5$ and $L(\alpha = 0) = +3.8$ for $Le = 2.0$.

where Le' is the effective Lewis number defined as

$$Le'(\alpha, Le) = Le\bigg/\left[1-\alpha\int_0^{\infty}\left(\frac{1-e^{-Le\tau}}{1+\gamma e^{\tau}}\right)d\tau\right] \tag{26}$$

Therefore, it is expected that the influence of Soret diffusion and Lewis number on Markstein length can be represented by the effective Lewis number Le'. Figure 5 shows the ratio between Lewis number and effective Lewis number as a function of Soret diffusion coefficient. It is seen that for both light and heavy fuels, the ratio, Le/Le', decreases linearly with the increase of α. Unlike Fig. 4, Fig. 5 indicates that the influence of Soret diffusion on Le/Le' of heavy fuel with $Le = 2.0$ is much stronger than on that of light fuel with $Le = 0.5$. Equation (25) indicates that Markstein length, L, increases as the value of Le' increases since $-(Z/2 - 2\sigma + 1)$ is negative. For $Le = 2.0$, Fig. 5 indicates that Le' increases with α, and thereby $L(\alpha)$ also increases with α. For $Le = 0.5$, Fig. 5 indicates that Le' decreases with $|\alpha|$ and thereby $L(\alpha)$ also decreases with the increase of $|\alpha|$ (note that L is negative for $Le = 0.5$). Consequently, the results in Fig. 5 are consistent with those in Fig. 4.

Figure 6 plots the Markstein length as a function of effective Lewis number. The Markstein length predicted by Eq. (25) is the same as those from linear extrapolation at different values of Le and α. This confirms that the Markstein length L can be characterized by the effective Lewis number Le', which includes the influence of Soret diffusion.

The above discussion shows that Soret diffusion has great impact on Markstein length of light and heavy fuels. Since the ignition process strongly depends on the Markstein length [6,8,9], it is expected that the critical ignition condition is also affected by Soret diffusion. This is demonstrated in the following subsection.

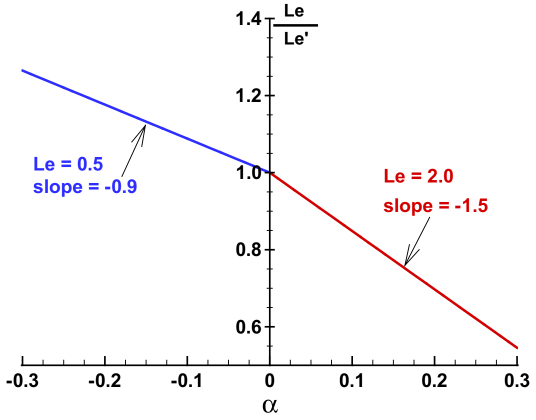

Fig. 5. The ratio between Lewis number and effective Lewis number as a function of Soret diffusion coefficient for $Le = 0.5$ and $Le = 2.0$.

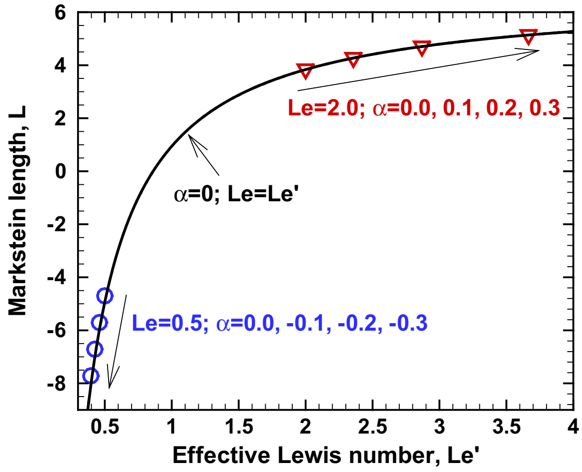

Fig. 6. The Markstein length as a function of effective Lewis number. Solid line: results from Eq. (25) for $\alpha = 0$ and thus $Le = Le'$; symbols: results obtained from linear extrapolation for $Le = 0.5$ and 2.0 with different values of α.

3.2. Influence of Soret diffusion on spherical flame initiation

In this sub-section we shall consider the ignition power deposition (i.e. $Q > 0$) and study the propagation of ignition kernel and critical ignition condition. Figure 7 shows the flame propagation speed as a function of flame radius at different ignition powers for heavy fuels ($Le = 2.0$) without and with Soret diffusion ($\alpha = 0$ and $\alpha = 0.1$). When there is no ignition power deposition at the center (i.e. $Q = 0$), the results are the same as those in Fig. 2(a) and only one flame branch of U–R exists. When a small external power is deposited at the center (lines 2 and 3 in Fig. 7), there exist two branches of solutions: the original traveling flame branch on the right and a new ignition kernel branch on the left. It is observed that the left and right branches move towards each other when the ignition power increases. When the ignition power is larger than the so-called minimum ignition power, Q_c, these two branches merge with each other, resulting in new upper and lower branches. Therefore, the ignition kernel can propagates outwardly along the upper branch, indicating that successful initiation is achieved. When Soret diffusion is neglected ($\alpha = 0.0$), the minimum ignition power is $Q_c = 1.931$. When Soret diffusion is considered ($\alpha = +0.1$), we have $Q_c = 3.205$. The minimum ignition power increases by 66% when Soret diffusion is taken into account. Therefore, Soret diffusion makes ignition become much more difficult for heavy fuels.

Figure 8 plots the normalized minimum ignition power, $Q_c(\alpha)/Q_c(\alpha = 0)$ as a function of Soret diffusion coefficient, α. For light fuels with $Le = 0.5$, the minimum ignition power decreases as the Soret diffusion intensity increases (from $\alpha = 0.0$ to $\alpha = -0.3$). The opposite holds for heavy fuels with $Le = 2.0$. Therefore, Soret diffusion makes ignition become more easy/difficult for light/heavy fuels. This is due to the facts that for light/heavy fuels, the flame intensities are pronouncedly improved/reduced by Soret diffusion and that both the critical flame radius and Markstein length decrease/increase when Soret diffusion is taken into account (see Figs. 2, 4 and 7).

Detailed numerical simulations were conducted for hydrogen/air flames without and with Soret diffusion [21]. For lean hydrogen/air, we have $\alpha < 0$. It was found that the absolute value Markstein length increases and the minimum ignition energy slightly decreases when the Soret diffusion is considered [21]. Therefore, the present theoretical results agree qualitatively with numerical simulation in [21].

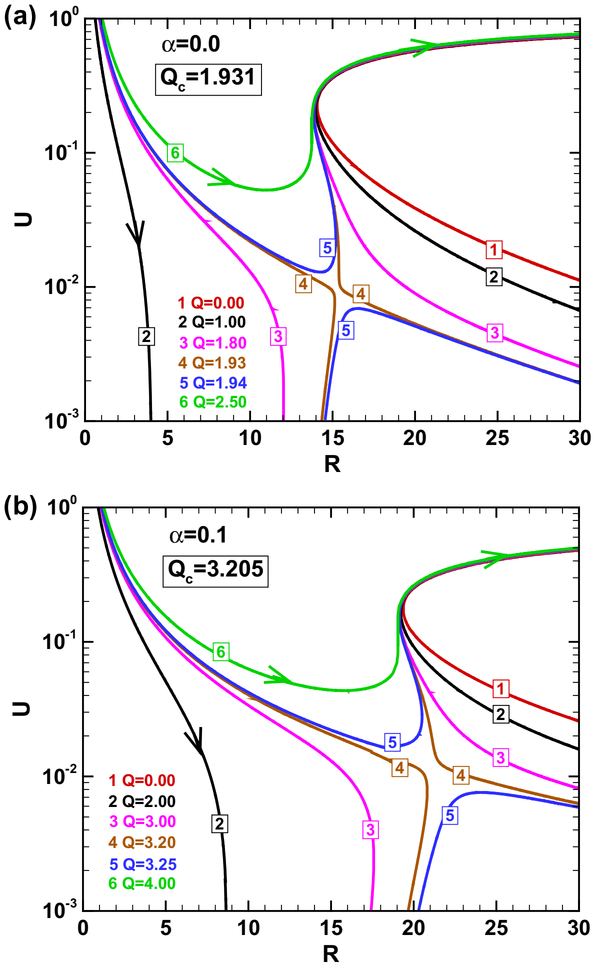

Fig. 7. Flame propagation speed as a function of flame radius at different ignition powers for $Le = 2.0$ with (a) $\alpha = 0$ and (b) $\alpha = 0.1$.

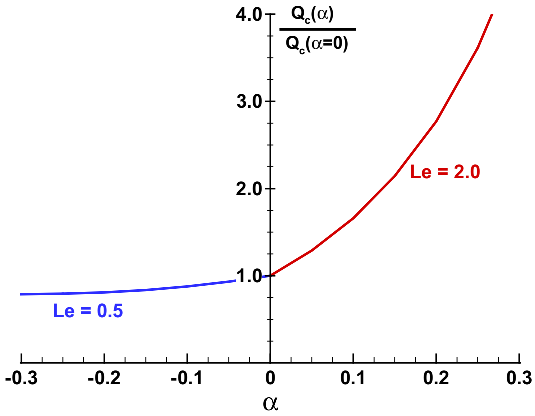

Fig. 8. The normalized minimum ignition power as a function of Soret diffusion coefficient. $Qc(\alpha = 0) = 0.0073$ for $Le = 0.5$ and $Qc\ (\alpha = 0) = 1.931$ for $Le = 2.0$.

Figure 6 and Eq. (25) indicate that the Markstein length L can be characterized by the effective Lewis number Le'. However, this does not hold for minimum ignition power. Figure 9 shows the minimum ignition energy as a function of effective Lewis number. When the Soret diffusion is neglected ($\alpha = 0$), we have $Le' = Le$ according to Eq. (26) and the results are represented by the black solid line in Fig. 9. We also consider the case of $Le = 2.0$ at different values of Soret diffusion coefficient of $\alpha = 0, 0.05, 0.1, \ldots 0.3$, for which the results are represented by the triangles in Fig. 9. It is observed that Q_c depends on not only Le' but also α. Therefore, unlike the Markstein length, the minimum ignition power cannot be solely characterized by the effective Lewis number. This is reasonable since the effective Lewis number given in Eq. (26) is obtained in the limit of $R \gg 1$ while the critical ignition condition is determined by the evolution of ignition kernel with $R \sim O(1)$.

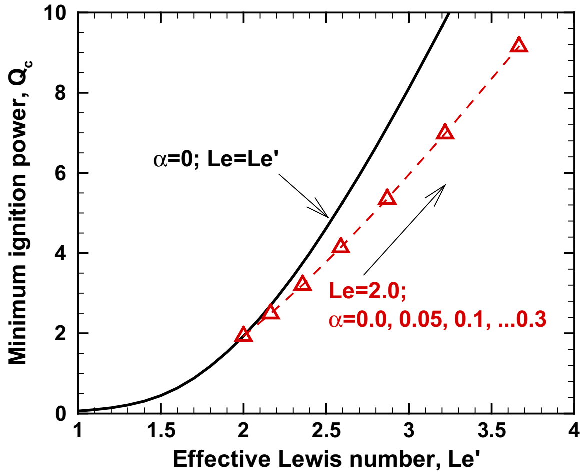

Fig. 9. Change of the minimum ignition power with effective Lewis number. Solid line: $\alpha = 0$, $Le = Le'$; symbols: $Le = 2.0$ with different values of α.

4. Conclusions

A theoretical model for spherical flame initiation and propagation with Soret diffusion is developed in this study. Large-activation-energy asymptotic analysis is conducted (the chemical source term is not solved, but is approximated by the corresponding jump conditions across the flame) and an analytical correlation between the flame propagation speed and flame radius is derived based on the quasi-steady assumption. With the help of this correlation, the effects of Soret diffusion on spherical flame propagation speed, Markstein length, and minimum ignition energy are assessed.

For spherical flame propagation, Soret diffusion strongly affects stretched flame speed and Markstein length. For light (heavy) fuels, Soret diffusion increases (decreases) the flame propagation speed and flame temperature. This is because Soret diffusion modifies the local equivalence ratio. The absolute value of Markstein length is shown to increase linearly with the magnitude of Soret diffusion coefficient, indicating that the stretched flame becomes more sensitive to stretch rate after including Soret diffusion. Furthermore, it is shown that the Markstein length can be characterized by an effective Lewis number which includes the influence of Soret diffusion.

For ignition process, Soret diffusion affects the minimum ignition power and makes flame initiation become easier (more difficult) for light (heavy) fuels. The minimum ignition power can be increased by more than 50% for $Le = 2.0$ after $\alpha = 0$ is changed to $\alpha = +0.1$. This indicates that the effect of Soret diffusion on the flame initiation is not negligible for hydrocarbon fuels with large Lewis number. Moreover, unlike the Markstein length, the minimum ignition power cannot be solely characterized by the effective Lewis number.

Conflict of interest

The authors declare that there are no conflicts of interest.

Acknowledgments

This work was supported by National Natural Science Foundation of China (Nos. 51322602 and 51136005) and Doctoral Fund of Ministry of Education of China (No. 20120001110080). We appreciate helpful discussions with Professor Chung K. Law and Mr. Wenkai Liang at Princeton University.

References

[1] P. Clavin, Dynamic behavior of premixed flame fronts in laminar and turbulent flows, Prog. Energy Combust. Sci. 11 (1985) 1–59.

[2] C.K. Law, Combustion Physics, Cambridge University Press, 2006.

[3] B. Deshaies, G. Joulin, On the initiation of a spherical flame kernel, Combust. Sci. Technol. 37 (1984) 99–116.

[4] M. Champion, B. Deshaies, G. Joulin, K. Kinoshita, Spherical flame initiation – theory versus experiments for lean propane-air mixtures, Combust. Flame 65 (1986) 319–337.

[5] P.S. Tromans, R.M. Furzeland, An analysis of lewis number and flow effects on the ignition of premixed gases, Proc. Combust. Inst. 21 (1988) 1891–1897.

[6] Z. Chen, Y. Ju, Theoretical analysis of the evolution from ignition kernel to flame ball and planar flame, Combust. Theor. Model. 11 (2007) 427–453.

[7] A.P. Kelley, G. Jomaas, C.K. Law, Critical radius for sustained propagation of spark-ignited spherical flames, Combust. Flame 156 (2009) 1006–1013.

[8] Z. Chen, M.P. Burke, Y. Ju, On the critical flame radius and minimum ignition energy for spherical flame initiation, Proc. Combust. Inst. 33 (2011) 1219–1226.

[9] H. Zhang, Z. Chen, Spherical flame initiation and propagation with thermally sensitive intermediate kinetics, Combust. Flame 158 (2011) 1520–1531.

[10] J.O. Hirschfelder, C.F. Curtiss, R.B. Bird, Molecular Theory of Gases and Liquids, John Wiley, 1954.

[11] A. Gomez, D.E. Rosner, Thermophoretic effects on particles in counterflow laminar diffusion flames, Combust. Sci. Technol. 89 (1993) 335–362.

[12] D.E. Rosner, R.S. Israel, B. La Mantia, "Heavy" species Ludwig–Soret transport effects in air-breathing combustion, Combust. Flame 123 (2000) 547–560.

[13] A. Ern, V. Giovangigli, Thermal diffusion effects in hydrogen–air and methane–air flames, Combust. Theor. Model. 2 (1998) 349–372.

[14] A. Ern, V. Giovangigli, Impact of detailed multicomponent transport on planar and counterflow hydrogen/air and methane/air flames, Combust. Sci. Technol. 149 (1999) 157–181.

[15] F. Yang, C.K. Law, C.J. Sung, H.Q. Zhang, A mechanistic study of Soret diffusion in hydrogen–air flames, Combust. Flame 157 (2010) 192–200.

[16] Y. Xin, C.-J. Sung, C.K. Law, A mechanistic evaluation of Soret diffusion in heptane/air flames, Combust. Flame 159 (2012) 2345–2351.

[17] H. Bongers, L.P.H. De Goey, The effect of simplified transport modeling on the burning velocity of laminar premixed flames, Combust. Sci. Technol. 175 (2003) 1915–1928.

[18] F. Yang, H.Q. Zhang, X.L. Wang, Effects of soret diffusion on the laminar flame speed of n-butane-air mixtures, Proc. Combust. Inst. 33 (2011) 947–953.

[19] A.L. Sánchez, F.A. Williams, Recent advances in understanding of flammability characteristics of hydrogen, Prog. Energy Combust. Sci. 41 (2014) 1–55.

[20] W. Liang, Z. Chen, F. Yang, H. Zhang, Effects of Soret diffusion on the laminar flame speed and Markstein length of syngas/air mixtures, Proc. Combust. Inst. 34 (2013) 695–702.

[21] W. Liang, C.K. Law, Z. Chen, Role of Soret diffusion in the ignition of hydrogen/air mixtures by a heated kernel, in: 8th US National Combustion Meeting, 2013, paper # 070LT-0030.

[22] P. Garcia-Ybarra, P. Clavin, Cross-transport effects in nonadiabatic premixed flames, in: Proceedings of the 7th International Colloquium on Gasdynamics of Explosions and Reactive Systems, 1981, pp. 463–481.

[23] P. Garcia-Ybarra, C. Ncoli, P. Clavin, Soret and dilution effects on premixed flames, Combust. Sci. Technol. 42 (1984) 87–109.

[24] M. Arias-Zugasti, D.E. Rosner, Soret transport, unequal diffusivity, and dilution effects on laminar diffusion flame temperatures and positions, Combust. Flame 153 (2008) 33–44.

[25] D. Fong, J.K. Bechtold, C.K. Law, Asymptotic structure of laminar diffusion flames at high pressure, Phys. Fluids 24 (2012) 093602.

[26] F. Wu, W. Liang, Z. Chen, Y. Ju, C.K. Law, Uncertainty in stretch extrapolation of laminar flame speed from expanding spherical flames, Proc. Combust. Inst., in Press. http://dx.doi.org/10.1016/j.proci.2014.05.065.

[27] L. Qiao, C. Kim, G. Faeth, Suppression effects of diluents on laminar premixed hydrogen/oxygen/nitrogen flames, Combust. Flame 143 (2005) 79–96.

[28] L. Qiao, Y. Gu, W.J.A. Dahm, E.S. Oran, G.M. Faeth, A study of the effects of diluents on near-limit H_2–air flames in microgravity at normal and reduced pressures, Combust. Flame 151 (2007) 196–208.

[29] L. Qiao, Y. Gu, W.J.A. Dahm, E.S. Oran, G.M. Faeth, Near-limit laminar burning velocities of microgravity premixed hydrogen flames with chemically-passive fire suppressants, Proc. Combust. Inst. 31 (2007) 2701–2709.

[30] M.P. Burke, Z. Chen, Y. Ju, F.L. Dryer, Effect of cylindrical confinement on the determination of laminar flame speeds using outwardly propagating flames, Combust. Flame 156 (2009) 771–779.

[31] Z. Chen, M.P. Burke, Y. Ju, Effects of Lewis number and ignition energy on the determination of laminar flame speed using propagating spherical flames, Proc. Combust. Inst. 32 (2009) 1253–1260.

[32] Z. Chen, On the extraction of laminar flame speed and Markstein length from outwardly propagating spherical flames, Combust. Flame 158 (2011) 291–300.

[33] S. Kwon, L.K. Tseng, G.M. Faeth, Laminar burning velocities and transition to unstable flames in $H_2/O_2/N_2$ and $C_3H_8/O_2/N_2$ mixtures, Combust. Flame 90 (1992) 230–246.

[34] E. Varea, J. Beeckmann, H. Pitsch, Z. Chen, B. Renou, Determination of burning velocities from spherically expanding H_2/air flames, Proc. Combust. Inst., in Press. http://dx.doi.org/10.1016/j.proci.2014.05.137.

[35] L. Courty, K. Chetehouna, Z. Chen, F. Halter, C. Mounaïm-Rousselle, J.-P. Garo, Determination of laminar burning speeds and Markstein lengths of p-cymene/air mixtures using three models, Combust. Sci. Technol. 186 (2014) 490–503.

[36] M. Metghalchi, J.C. Keck, Laminar burning velocity of propane–air mixtures at high temperature and pressure, Combust. Flame 38 (1980) 143–154.

[37] C.J. Rallis, A.M. Garforth, The determination of laminar burning velocity, Prog. Energy Combust. Sci. 6 (1980) 303–329.

[38] S.D. Tse, D.L. Zhu, C.K. Law, Morphology and burning rates of expanding spherical flames in H_2/O_2/inert mixtures up to 60 atmospheres, Proc. Combust. Inst. 28 (2000) 1793–1800.

[39] X. Qin, Y. Ju, Measurements of burning velocities of dimethyl ether and air premixed flames at elevated pressures, Proc. Combust. Inst. 30 (2005) 233–240.

[40] G. Joulin, P. Clavin, Linear stability analysis of nonadiabatic flames: diffusional-thermal model, Combust. Flame 35 (1979) 139–153.

[41] Y. Wu, Z. Chen, Asymptotic analysis of outwardly propagating spherical flames, Acta Mech. Sin. 28 (2012) 359–366.

[42] A. Veeraragavan, C.P. Cadou, Flame speed predictions in planar micro/mesoscale combustors with conjugate heat transfer, Combust. Flame 158 (2011) 2178–2187.

[43] L. He, Critical conditions for spherical flame initiation in mixtures with high Lewis numbers, Combust. Theor. Model. 4 (2000) 159–172.

[44] R.M. Fristrom, L. Monchick, Two simple approximations to the thermal diffusion factor and their applications to flame studies, Combust. Flame 71 (1988) 89–99.

[45] Z. Chen, X. Gou, Y. Ju, Studies on the outwardly and inwardly propagating spherical flames with radiative loss, Combust. Sci. Technol. 182 (2010) 124–142.